

Flow curves estimation of aqueous solutions of hydrocolloid mixtures: Xanthan and Tara gum

¹*Miranda-Zanardi L. F., ²Miranda-Medina J. F., ¹Medina-Lezama E. A. *Chemical Eng. Department, Universidad Nacional de San Agustín de Arequipa. Santa Catalina 117, Arequipa, Peru 04001*

Mechatronic Eng. Department, Universidad Católica San Pablo. Campus San Lázaro – Quinta Vivanco s/n, Arequipa, Peru 04001

Abstract

Tara gum has an increasing demand as a texture agent. Its rheological properties can be significantly improved by combining it with other hydrocolloids such as Xanthan. The mixture of aqueous solutions of Tara gum and Xanthan show a pseudoplastic behavior with a clear synergy effect presenting maximum viscosity values. In this work, we propose a reliable strategy for the estimation of flow curves of mixtures of hydrocolloids aqueous solutions.

Upon testing several alternatives, the Herschel and Bulkley model was selected to fit the flow curves of Tara gum and Xanthan aqueous solutions, as well as their mixtures, since this model provided a high correlation coefficient. The next step proposes a set of key equations to establish quantitative relations between the parameters of the Herschel and Bulkley model and the composition variables of the mixtures. A simple equation based on only two experimental points was developed to estimate yield stress. In addition, the Auslander model and Chebyshev polynomials were successfully applied to correlate consistency index to composition. The flow index was determined by means of linear functions. Also, in order to improve the overall estimation, the error was reduced from 9.72 % to 2.59 % upon applying optimization routines. The accuracy achieved by the proposed strategy can have an immediate impact on an industrial scenario, since the user may tailor desired viscosity properties by adjusting the composition variables. Hence, a consistent procedure has been developed to estimate flow curves for mixtures that show important synergy effects.

Keywords

Flow curve estimation, Tara gum, Xanthan, hydrocolloids mixture

Nomenclature

η	Viscosity [Pa.s]
η_{exp}	Experimental viscosity [Pa.s]
η_0	Zero shear rate viscosity [Pa.s]
η_{∞}	Infinite viscosity (at 1000 s^{-1}) [Pa.s]
\square	Shear stress [Pa]
\square_0	Yield stress [Pa]
σ_{36}	Estimated Yield Stress [Pa]
σ_s	Surplus stress [Pa]
\square	Shear rate [s^{-1}]
x	Mass fraction
k	Consistency index [Pa s^n]
n	Flow index
λ	Time constant, Cross Eq. [s]
E_{η}	Enhancement viscosity coefficient
I_{η}	Synergy interaction index
α	Intermolecular cohesion parameter
G_{12}	Grunberg & Nissan parameter

Introduction

Hydrocolloids or gums are biopolymers typified as polysaccharides. They are texture agents that have found wide use in food and many other industrial sectors (Contreras-Lozano *et al.*, 2018; Shaari *et al.*, 2017). This is due to their ability to act as thickening, gelling or emulsifying solutions at relatively low concentrations (Alghooneh *et al.*, 2019).

Xanthan gum is an extracellular polysaccharide secreted by the *Xanthomonas Campestris* microorganism. This gum has a primary structure composed of D-glucose units linked together by 1-4 bonds, which contains branches formed by D-mannose - 1,4 - Dglucuronic acid -1, 2 - d-mannose. It may also contain pyruvic acid and acetic acid. It is considered an anionic polymer due to the presence of carboxylic groups in its structure (Gulrez *et al.*, 2012). Xanthan gum is soluble in cold water and its solutions exhibit a markedly pseudoplastic behavior. Its viscosity has excellent stability over a wide range of pH and temperature values, and the polysaccharide is resistant to enzymatic degradation (Valenta *et al.*, 2018).

Tara Gum is derived from the endosperm of the Tara plant, *Caesalpinia Spinosa*, which is native to Peru, having a growing demand (EFSA, 2017). Tara gum belongs to the family of the galactomannans and is formed by a main chain of mannose with branches of galactose every three mannoses. The molecular weight of Tara gum is 1.159×10^6 g/mol and the polydispersity index has the value of 1.154 (Wu *et al.*, 2017). The aqueous solutions of Tara gum exhibit high viscosity which is relatively stable to electrolytes but decreases at low pH and high temperature (Wu *et al.*, 2015; Sittikijyothin *et al.*, 2005).

Synergistic interactions between Xanthan gum and galactomannans such as Guar or Tara gum in aqueous solutions have been reported (Ramos and Hernandez, 2020). This synergy is shown as viscosity increments at low concentrations; while, at high concentrations, soft gels are formed (Fitzsimons *et al.*, 2008). In a pioneering work Tako (1991) proved that there is a synergistic interaction between Xanthan gum and Tara gum aqueous solutions, concluding that the side chains of the Tara gum molecule reduced interaction with Xanthan gum.

The mixtures of xanthan gum and galactomannans aqueous solutions finds several applications, for example for curcumin formulations (Da Lozzo, 2013) and for drug delivery (Kennedy *et al.*, 2015). Xanthan gum solutions behaved as weak gels, whereas guar gum solutions suggest the presence of entanglement and the formation of a viscoelastic gel-like structure, when both gums are mixed together (Martin-Alfonso *et al.*, 2018). The limited miscibility of biopolymers is responsible for synergistic or antagonistic effects (Alghooneh *et al.*, 2019).

This work addresses the development of a strategy to reliably estimate the flow curves of mixtures of hydrocolloids aqueous solutions. For that purpose, experiments were conducted to determine flow curves of Xanthan and Tara gum mixtures of aqueous solutions. Based on the experimental evidence the synergy was evaluated. The Herschel & Bulkley model was applied to represent the flow curves of individual experiments. Several methods were applied to determine the parameters of this model. In order to estimate viscosity corresponding to new values of composition, it is necessary to correlate the Herschel and Bulkley model parameters to composition. But this is a difficult task, since the synergy effect developed by the interaction of these gums, causes complex profiles that describe the variation of the parameters to composition.

Estimation of Mixtures Viscosity

Rheology studies the flow and deformation of materials under external stress, especially those that cannot be described by simple linear models of hydrodynamics and elasticity (Picout and Ross-Murphy, 2003). According to their nature rheological models can be classified as theoretical, structural and empirical (Rao, 2014). Apparent viscosity is the quotient of shear stress over shear rate, Eq. 1. Flow Curve is the experimental correlation of shear stress to shear rate. Pseudoplastic fluids decrease their viscosity values while the shear rate is augmented and show an almost linear profile for flow curves. For pseudoplastic fluids, at high shear rates, apparent viscosity reaches a small constant value (η_∞); on the contrary, if shear rate tends to zero its value is called the “zero shear viscosity” η_0 .

Table 1. Some Viscosity Models

Purpose	Model	Reference	Eq.
Viscosity definition	$\eta = \sigma / \dot{\gamma}$		1
definition			
Power law flow curves	$\dot{\gamma} = k \sigma^n$	Eberhard 20193	
Flow curves	$\sigma = \sigma_0 + k \dot{\gamma}^n$	Herschel and Bulkley 1929	4

Flow curves. Modified Herschel & Bulkley		$\sigma = \sigma_0 + \sigma_s(\gamma/\gamma_s)^n$	Saasen and Ytrehus 2018	5	$\eta_a = \frac{\eta_0 - \eta}{\eta_0 - \eta_\infty}$
Yield stress, σ_0 . Parabolic fit Dimensionless Viscosity		$\sigma_0 = A_0 + A_1\gamma + A_2\gamma^2$		6	
		$\sigma_{36} = 2\sigma_3 - \sigma_6$	Yield Stress, σ_{36} . Zamora and		
Linear fit Power 2002	7	$\eta = \eta_\infty + \frac{\eta_0 - \eta_\infty}{1 + (\lambda\gamma)^{1-n}}$	Viscosity curves. Cross 1979		
8		$\eta = \eta_\infty + (\eta_0 - \eta_\infty)\exp(-k\gamma)$	and Ibarz 2010		
Viscosity difference for mixtures Cross model Viscosity curves		$I_\eta = \frac{\Delta\eta}{x_1\eta_1 + x_2\eta_2}$	Gayathri et al. 2019	10	
		$E_\eta = \frac{2\eta_{max}}{(\eta_1 + \eta_2)} - 1$	Falguera Synergy Belda et al.	9 11	
Interaction Index 2004 Enhancement Modified	12	$\Delta\eta = x_1x_2 \sum_{i=0}^n A_i (x_1 - x_2)^i$	Coefficient from Belda et al. 2004		
polynomial expansion for mixtures	13		Viscosity Redlich and Kister 1948		
Viscosity of binary mixtures. 1 parameter		$\ln \eta = \frac{x_1}{x_1 + \alpha x_2} \ln \eta_1 + \frac{\alpha x_2}{x_1 + \alpha x_2} \ln \eta_2$	Zhmud 2014	15	binary mixtures.
Lederer- Roegiers 1 parameter		$\alpha = \frac{\ln \left[\frac{\eta_{12}}{\eta_1} \right]}{\ln \left[\frac{\eta_2}{\eta_1} \right]}$	Intermolecular cohesion parameter		
Viscosity of binary mixtures. Auslander 3 parameter model		$\eta = \frac{x_1\eta_1(x_1 + B_{12}x_2) + x_2\eta_2A_{21}(B_{21}x_1 + x_2)}{x_1(x_1 + B_{12}x_2) + x_2A_{21}(B_{21}x_1 + x_2)}$	Auslander, 1964	16	
Chebyshev $p_n(x) = \sum_{i=0}^n a_i T_i(x)$ being $T_0 = 1, T_1 = x, T_n(x) = 2xT_{n-1}(x) - T_{n-2}(x)$	Kim, 2014		17		

The Herschel and Bulkley model (1926), Eq. 4 presented in Table 1, is widely used to correlate flow curves (Salehi and Kashaninejad, 2017). When the yield stress (σ_0) is negligible, Eq. 4 simplifies to the Power Law, Eq. 3. On the other hand, to correlate experimental viscosity data in terms of shear rate the Cross model (Moraes *et al.*, 2011) is widely used, Eq. 8. Alternative models have been proposed by Falgera and Ibarz (2010) and by Kazunori (2006).

The viscosity of liquids depends on both the collision among the particles and the force fields that determine the interactions between the molecules. Therefore, the theoretical description of viscosity is complex (Ahmad *et al.*, 2013). A fairly common working procedure to estimate the viscosity of mixtures is to calculate the differences between the experimental values, η_{exp} , and those that would be obtained if the mixtures exhibited a linear behavior. For binary mixtures, such differences may be represented by Eq. 10. Polynomial expansion 13 is applied to adjust these differences by the least squares technique (Redlich and Kister, 1948), where $\Delta\eta$ stands for the Excess Viscosity, or synergy effect. From this approach, Grunberg and Nissan (1949) derived a phenomenological

model, Eq. 14, considering a single adjustable parameter G_{12} , which is proportional to the exchange energy and can be considered as an indicator of the non-ideal behavior of binary mixtures.

Several other equations have been developed to estimate the viscosity of mixtures. The Auslander model (1964), Eq. 16 contains three adjustable parameters (A_{21} , B_{12} , B_{21}) and has shown a better fit than previous models (Knežević-Stevanović et al., 2012). Chebyshev polynomials approximate well an arbitrary function $f(x)$ by Eq. 17. This set of polynomials $T_n(x) = \cos n\theta$, for $n=0, 1, \dots, 8$ is generated from the sequence of cosine functions using the transformation $\theta = \cos^{-1} x$ which is valid for a real value of x ranging from -1 to 1. Chebyshev polynomials offer several advantages like simple determination of the zeros and extrema points, as well as reduction of the error by the minimax best fit criterion (Thompson, 1994). Of course, there is a compromise between the complexity of the equation and the goodness of fit.

The power law, Eq. 3, has been used to fit the flow curves of Tara gum (Wu *et al.*, 2015) and mixtures of Xanthan gum and pectin aqueous solutions (Soto-Caballero *et al.*, 2016). Zhmud (2014) proposes the use of the Lederer-Roegiers Eq. 15, in order to fit the viscosity data of hydrocarbon mixtures.

Materials and methods

The flow curves of mixtures of aqueous solutions of Tara gum and Xanthan have been determined. The materials used for the preparation of solutions were: Tara gum provided by “Somerec Mercantil Company”, lot 01008; and, Xanthan Keltrol F gum, provided by “Montana Corporation”, lot 485.

To prepare 4 g/L stock aqueous solutions of Tara and Xanthan gums in distilled water, the gums were weighed in an analytical balance Ohaus EX225D and dissolved at 40 ° C using a rotation speed of 2000 rpm. The solutions were heated at 80 ° C for 15 minutes, afterwards they were allowed to cool down and finally were stored for 24 hours at approximately 6 ° C, before use. Gum solutions were processed in a two-liter stainless steel tank by means of a mechanical agitator IKA EuroStar 60 coupled to a water bath Julabo Corio BC4. A Rushton turbine was used as impeller.

Afterwards the mixtures of aqueous solutions of Tara and Xanthan gums were prepared, corresponding to the following Tara gum mass fractions: 0.0; 0.1; 0.2; 0.3; 0.4; 0.5; 0.6; 0.7; 0.8; 0.9 and 1.0. The above mixtures were obtained at total concentrations of 1.0; 2.0; 3.0; and 4.0 g/L by dilution with distilled water.

Viscosity and shear stress were measured using an Anton Paar MCR 702 rotational rheometer at shear rate values ranging from 0.1 to 1000 s⁻¹ and keeping temperature constant at 25 ° C. Samples were placed in a double couette device Standard Measuring System DG26.7/T200/SS attached to the rheometer and linked to a computer operated by means of the software RheoCompass.

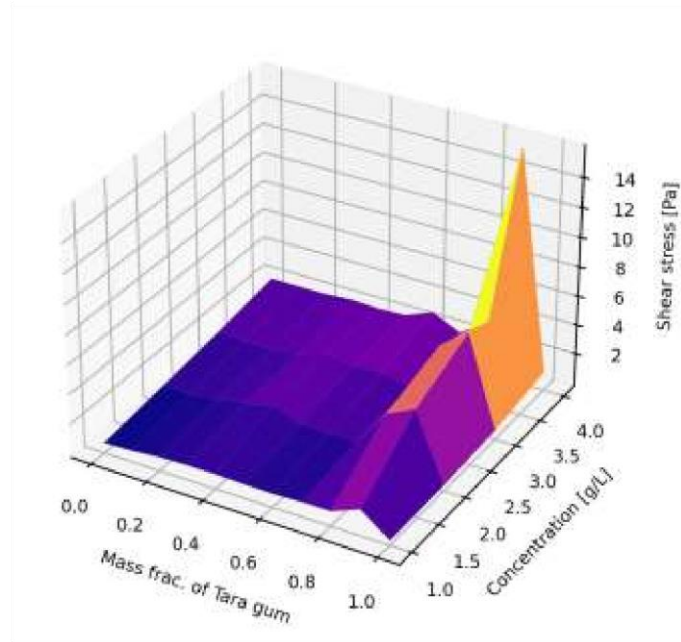
Processing the experimental results requires the application of the Herschel and Bulkley model to determine its parameters and the goodness of fit. Most calculations were performed using a spreadsheet while the optimization of the main models applied the routine “scipy.optimize.least_squares” programmed in Python (2021). This module has three algorithms to perform minimization. The Dogleg algorithm with rectangular trust regions was selected because it is used for small problems with bounds.

A next step requires the correlation of the consistency index (k) to composition, by means of several models, like Auslander and Chebyshev. Then, the flow index (n) is computed using an empirical equation that has two independent variables: k and total concentration (C_T).

Results and discussion

The mixtures viscosity, and therefore the shear stress, of aqueous solutions of Xanthan and Tara gum present a complex relation to composition. Figure 1(A) shows the shear stress (Pa) surface at a constant shear rate of 9.03 s⁻¹ in terms of two independent variables: total concentration (C_T , g/L) and mass fraction of Tara gum (X_{Tara}).

1(A)



1(B)

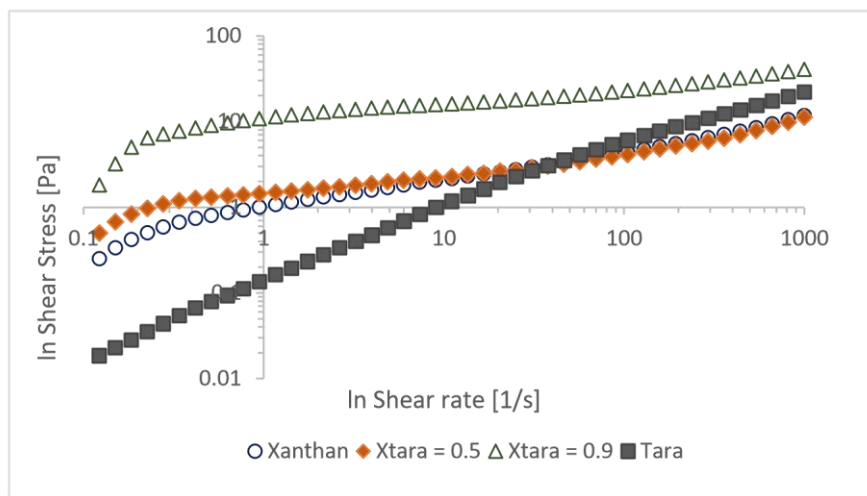


Figure 1. Variation of Shear Stress in terms of Composition.

(A) Surface at 9.03 s^{-1} shear rate. (B) Selected Flow Curves

As observed, the surface is very irregular indicating significant interactions among the gums. At X_{tara} close to 0.9, shear stress attains its maximum values; also, at higher concentration of gums in the mixture, the shear stress increases. Therefore, the largest shear stress value corresponds to $C_T = 4 \text{ g/L}$ and $X_{tara} = 0.90$.

Figure 1(B) presents selected flow curves for 4 g/L total concentration solutions, corresponding to pure Xanthan, pure Tara gum and their mixtures that contain 0.5 and 0.9 mass fraction of Tara gum. The curves show quasi-linear profiles on a double- logarithmic scale, therefore the solutions and their mixtures are categorized as pseudo-plastic fluids. At shear rate below 20 s^{-1} , Tara gum has the lowest shear stress, but its slope is higher than the ones corresponding to other samples.

The higher shear stress values belong to the $X_{tara} = 0.9$ curve, followed by the one of $X_{tara} = 0.5$. For Xanthan and Guar gum mixture of aqueous solutions with a 0.1% total polysaccharide concentration, a maximal viscosity value was achieved at the 0.6 mass fraction (Secouard *et al.*, 2007); while Amundarain *et al.* (2009) reported for the same mixture that maximum viscosity was obtained at 0.85 or 0.90 guar mass fraction. For mixtures of Xanthan gum and galactomannans, like guar gum and locust bean gum, in a 1% w/w solution, maximum elasticity corresponded to a 0.5 mass fraction (Jo *et al.*, 2018). Razavi and his team (2018) indicates that the best synergistic mixtures of Sage seed gum and Xanthan gum are for a 0.75 mass fraction. Thus, the location of the synergy effect depends on the components involved, their concentration and also the processing conditions (Gomez-Diaz *et al.*, 2008).

The mixture synergy effect

Table 1 presents two indicators of synergy: Synergy Interaction Index (I_η), Eq. 11, and Enhancement Coefficient (E_η), Eq. 12. I_η is defined as the quotient of the excess viscosity ($\Delta\eta$), Eq. 10, over the ideal viscosity. The Synergy Interaction Index for Shear Stress (I_σ) was computed replacing in Eq. 11 the shear stress values instead of the viscosity data. I_σ varied from about 14 to 26, at a shear

rate of 9.03 s^{-1} and $25 \text{ }^\circ\text{C}$, revealing high interaction among Tara gum and Xanthan. The maximum synergy is located at a Tara gum mass fraction of 0.9, regardless of total concentration. I_σ is inversely proportional to total concentration, since the values of the 1 g/L and 2 g/L series are higher than those of the 3 g/L and 4 g/L series.

The antagonism or synergism effects of food biopolymers is caused by their limited miscibility at the molecular level (Alghooneh et al., 2019). Tako *et al.* (2010) proposed an interaction mechanism between Xanthan gum and Galactomannans by the establishment of binding sites for D-mannose-specific interaction by means of hydrogen bonding and van der Waals interactions.

Wu *et al.* (2012), concluded that the synergistic interactions between galactomannans and cellulosic polysaccharides are generated by side groups that contribute with forming “hyper entanglements” which could increase viscosity; while the stiffer chains with more unsubstituted regions can form junction zones with the cellulosic molecules.

Yield stress

In order to fit the experimental data to known models it is necessary to determine characteristic magnitudes. For example, the Herschel & Bulkley model, Eq. 4, includes the yield stress; while the viscosity models, Eqs. 8 and 9, present the Zero Shear Viscosity and the Infinite Viscosity. Even though the calculation of these parameters is straightforward, it is necessary to define clear computational procedures.

Determination of the yield stress has several choices. Souza and Dutra (2004), stated that the yield stress becomes evident in the flow curves, because of the plateau or almost constant shear stress values presented. Allouche *et al.* (2015) propose an electrocapillarity technique for its precise determination. Figure 1(B) shows clearly that pure Tara gum solution does not have such a shear stress plateau and consequently its yield stress is negligible. On the opposite, the solution of Xanthan gum and its mixtures with Tara gum, exhibit a steep change in slope, the so-called shear stress plateau, when the shear rate values are below 1.0 s^{-1} , which indicates the presence of the yield stress.

In this work, the yield stress (σ_0) has been determined by three methods. The first method fits a second order polynomial, equation 6, to ten points with shear rate values varying from 0.95 to 5.99 s^{-1} ; where the estimated yield stress is the independent coefficient (A_0). The second method was developed modifying Eq. 7, proposed by Zamora and Power (2002), to Eq. 18:

$$\sigma_{39} = 2\sigma_3 - \sigma_9 \quad (18)$$

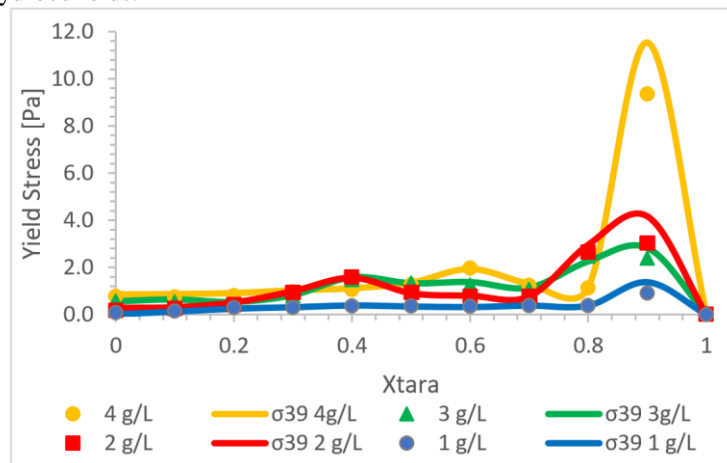
where σ_3 and σ_9 are the shear stress values (Pa) corresponding to the 3.0 and $9.0 \text{ (s}^{-1})$ shear rate values; and, the estimated yield stress is represented by σ_{39} . The third method applies an optimizer to the Herschel & Bulkley model having as objective function the minimization of the residual squares, and the calculated yield stress is represented by $\sigma_{0,opt}$.

The correlation coefficients of the yield stress values computed by fitting Eq. 6 and the ones calculated by means of Eq. 18, were higher than 0.98, demonstrating that both methods estimate approximately the same values. The optimized yield stress values were always higher than the ones calculated by Eq. 6, showing an average deviation about 11 % for higher concentrations, but for 1 g/L the deviation is close to 40 %. Such deviations were computed with the following equation:

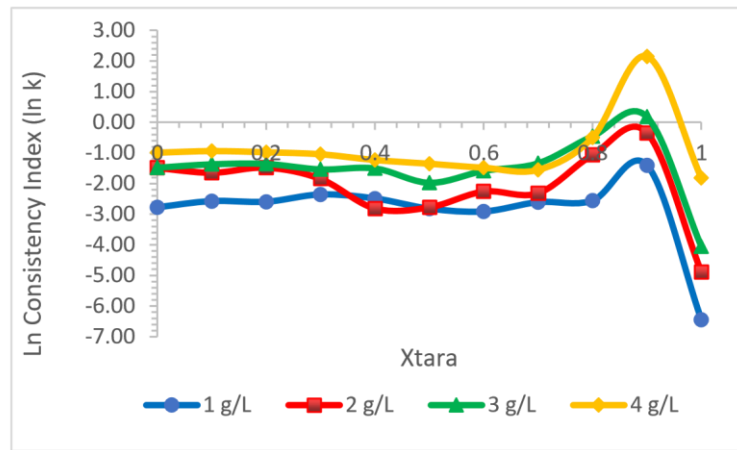
$$D_{opt} = 100 \frac{\sum(\sigma_{0,opt} - \sigma_0)^2}{\sum \sigma_0^2} \quad (19)$$

Figure 2 (A) represents the changes of the Yield Stress in terms of two composition variables: X_{tara} and C_T . Lines represent the yield stress (σ_{39}) values calculated by Eq. 18 and dots correspond to the yield stress determined by Eq. 6 (σ_0). As mentioned before, there is a close agreement between the yield stress computed by both models, which highlights the usefulness of Eq. 18 due to its accuracy and simplicity. It is observed that an increase in total concentration results in a higher yield stress. Moreover, it is evident that the mixtures of Tara gum and Xanthan show higher yield stress values than the pure components. This fact is one more evidence of the synergy effect between both hydrocolloids.

2(A)



2(B)



2(C)

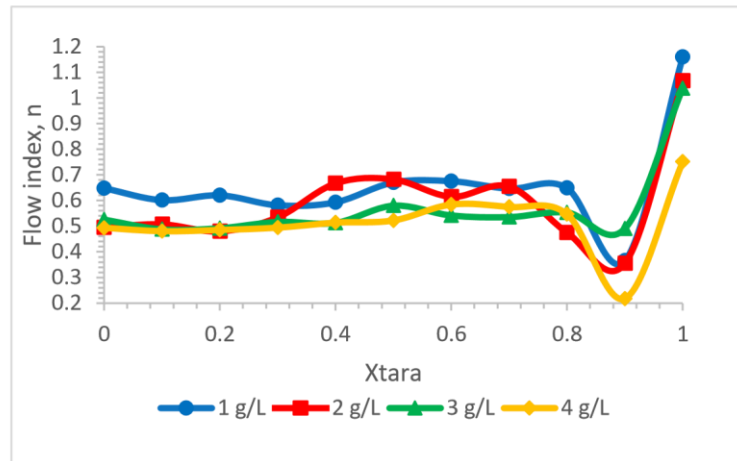


Figure 2. Herschel and Bulkley parameters composition dependence.

(A) Yield Stress; (B) Consistency Index; (C) Flow Index

The Herschel & Bulkley model

To estimate viscosity the flow curves may be correlated by means of the Herschel & Bulkley model, Eq. 4, or with the modification proposed by Saasen and Ytrehus (2018), Eq. 5. Another possibility is to fit viscosity curves using the Cross model, Eq. 8, or the model proposed by Falguera and Ibars (2010), Eq. 9. This last model did not offer an acceptable fit. In the case of mixtures, the parameters modify their values in agreement with composition variables: total concentration and Tara gum mass fraction. It is desirable to correlate such parameters to composition by simple models, but if the Synergy Interaction Index presents high values, the curve fit requires models with several parameters.

The Herschel and Bulkley model (1926), Eq. 4, is used extensively to fit experimental flow curves due to its simplicity and precision. Three parameters describe the flow curves: yield stress (σ_0 , Pa), consistency index (k , Pa sⁿ) and flow index (n). The procedures to calculate the yield stress have been previously described.

In order to determine the values of k and n , Eq. 4 has been linearized:

$$\ln(\sigma - \sigma_0) = \ln k + n \ln \dot{\gamma} \quad (20)$$

Shear rate – shear stress data pairs ranging from 0.95 to 1000 s⁻¹ were taken into account for the computation of k and n . The correlation coefficients for such fits were near 0.99, except for the mixtures that had X_{tara} close to 0.9, since they dropped to about 0.94, due to an increase in the non-linear behavior of the flow curves, as shown in Figure 1(B). An alternative procedure to calculate the values of k and n is to apply an optimization routine to the experimental data. This work uses the *Scipy optimize* least squares optimization module developed in Python (Scipy.org, 2021).

The consistency index (k) depends on composition and presents a wide range of variation. The values obtained by means of Eqs. 6 and 20 change from 0.02 to 8.587 Pa.sⁿ. For example, the k maximum value at a C_T of 1 g/L is 0.245 while at 4 g/L the value raises to 8.597 Pa.sⁿ. Figure 2 (B), represents the effect of X_{tara} and C_T , on the logarithm of k , and it is observed a maximum $\ln k$ value located at X_{tara} of 0.90.

The flow index (n) is an indicator of the non-Newtonian character of liquids. Figure 2(C) shows that Tara gum solutions exhibit a Newtonian pattern for concentrations equal to or below 3 g/L; but Xanthan gum presents a pseudoplastic behavior with n about 0.6. The mixtures of Tara gum and Xanthan do not change much the n values, except when $X_{tara} = 0.9$ where a minimum is located, indicating that the pseudoplastic character gets more pronounced. The results from applying Eqs. 6 and 20 showed that n varies from 0.217 (pseudoplastic) to 1.160 (dilatant). The lowest value corresponds to the 4 g/L mixture having X_{tara} equal to 0.9; while the highest value corresponds to 1 g/L pure Tara gum.

Eq. 12 presents an Enhancement Coefficient (E_i) adapted to mixtures of solutions from the definition of Belda *et al.* (2004). Enhancement coefficients of the logarithm of the consistency index ($\ln k$) and the flow index (n) reveal that they depend on total concentration. The variation of $\ln k$ is much bigger than the one corresponding to n , since for a total concentration of 4.0 g/L $E_{\ln k} = 2.53$, while $E_n = 0.65$.

Consistency Index and Flow Index estimation

In order to correlate the data of Figure 2(B), $\ln k$ versus X_{tara} , the following models have been tested: Grunberg and Nissan, Eq. 14; Lederer- Roegiers, Eq. 15; Auslander, Eq. 16; Redlich & Kister, Eq. 13; and Chebyshev polynomials, Eq. 17. Due to the maximum values presented in Figure 2 (B), single parameter models were not suitable (i.e., Eqs. 14 and 15). Some modifications have been proposed to improve the Grunberg and Nissan model (Lapuerta *et al.*, 2017; Roegiers and Zhmud, 2011).

The Auslander model (3 parameters), Eq. 16, achieves better results correlating $\ln k$ to X_{tara} than the Redlich & Kister expansion (4 or more parameters). Chebyshev polynomials, however, showed a better estimation than the Auslander model.

The parameter B_{12} of the Auslander model has a constant value of -3.00; parameter A_{21} has a value close to -4.90 varying slightly with concentration; but, parameter B_{21} is linearly dependent on concentration. The correlation coefficients (R^2) relate the values of $\ln k$ determined from the experimental flow curves with the ones computed by the Auslander Model, showing an average of 0.960. So, the Auslander model is a good choice for this task. Definitely the Chebyshev polynomials achieved a better correlation. For a given C_T value, the Flow Index (n) of the Herschel and Bulkley model was calculated by a straight line that has k as independent variable. Thus, the relation between $\ln k$ and n is accurately represented by Eq. 21. The coefficients a_{00} , a_{01} , a_{10} and a_{11} were computed by regression from the experimental data.

$$n = (a_{00} + a_{01}C) + (a_{10} + a_{11}C)\ln k \quad (21)$$

Accordingly, the following procedure is suggested to calculate the Herschel and Bulkley parameters (σ_0 , k and n):

1. Calculate the yield stress using Eq. 18 ($\sigma_{3\theta}$) or Eq. 6 (σ_0). Another choice is to apply an optimization routine to estimate the three parameters of the model simultaneously ($\sigma_{0,opt}$, k and n) having as objective function the minimization of the residual sum of squares.
2. By means of Eq. 20 determine k and n . Another option is to apply the optimization routine mentioned in step 1.
3. Fit the $\ln k$ values corresponding to the X_{tara} data by means of a model like Auslander or Chebyshev.
4. Calculate the value of n applying Eq. 21.
5. Compute with these parameters the corresponding shear stress values and the summation of the square deviations in order to find the estimation error.

Fitting flow curves allows the estimation of viscosity values considering the following independent variables: shear rate (γ), X_{tara} and C_T . The average correlation coefficient of such estimation for the concentration of 4 g/L is 0.997.

Error Analysis

As stated previously, the estimation of shear stress or viscosity requires several stages, and on each stage an estimation error occurs. It is necessary to determine the total error. The error is computed by means of the following equation:

$$Error = 100 \frac{\sum(\sigma_{est} - \sigma)^2}{\sum \sigma^2} \quad (22)$$

Being σ the experimental shear stress and σ_{est} the calculated value. The error vector applies Eq. 22 to the 3D matrices for each of the four concentrations separately. The optimization of the parameters of the Herschel and Bulkley model was carried out with the *scipy.optimize* toolbox. For a given data set of the form $\{x_{data}, y_{data}\}$, let the function F with a set of parameters A be the fit function that estimates $y_{est} = F(x_{data}, A)$ where y_{est} is an estimate of y_{data} . The Herschel and Bulkley model corresponds to function F , consequently the set of parameters A are $\{\sigma_0, k, n\}$, x_{data} and y_{data} represent the shear rate (γ) and the shear stress (σ) values, respectively.

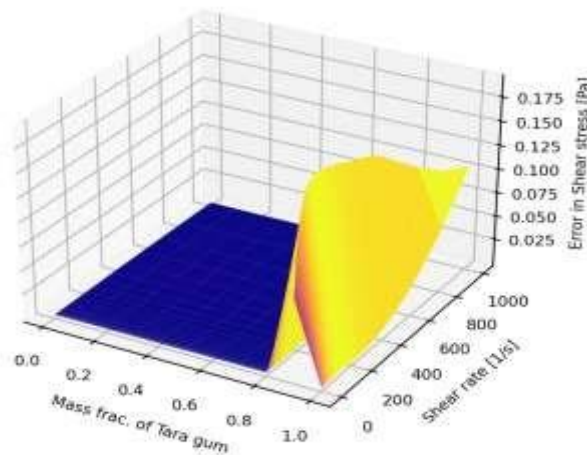
Table 2 presents the most representative cases. The first two columns under the heading "Individual values" indicate the procedure to calculate the Herschel and Bulkley parameters for each experiment, having as independent variables X_{tara} and C_T . The third and fourth column, named "Serial values" report the method used to fit the series of consistency index (k) in terms of X_{tara} for a fixed C_T .

Table 2. Error Analysis

Case Number	Individual values		Serial values		Error
	Yield Stress	k and n	k	n	%
1	Eq 6	Eq 20			8.105
2	Eq 6	Opt			0.160
3	Eq 18	Opt			0.137
4	Opt	Opt			0.086
5	Eq 18	Opt	Auslander	Eq 21	9.722
6	Eq 18	Opt	Chebyshev	Eq 21	4.711

The first four cases report the error on the calculation of individual values of shear stress. Applying an optimization procedure, the Herschel and Bulkley model shows an excellent fit (0.086 %). Cases 2 and 3 indicate that the computation of the yield stress by Eq. 6 or 18, offers about the same result, which means that Eq. 18 is a good choice despite its simple application. It is important to observe that the yield stress value does not affect significantly the global error; but the value of n is greatly responsible for the accuracy of the computations. The correlation of the $\ln k$ values with X_{Tara} is better for the Chebyshev polynomials (case 6), but in many situations the Auslander model offers suitable estimations (case 5).

3(A)



3(B)

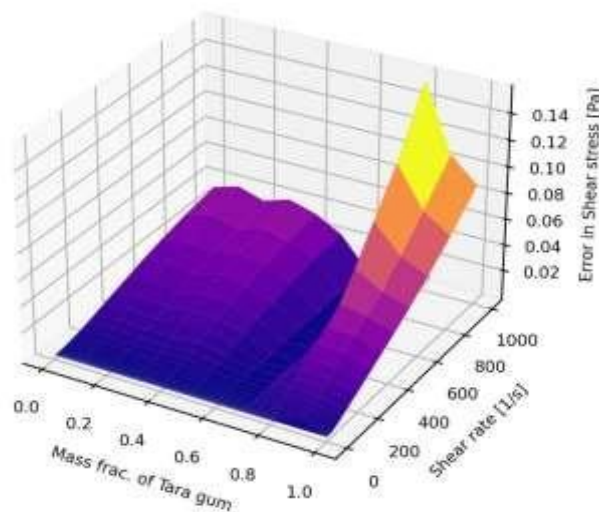


Figure 3. Shear Stress error for (A) Case 1 and (B) Case 6 of Table 2

Figure 3(A) presents the detail of the error, computed with Eq. 22, corresponding to the mixture that has a C_T value of 4.0 g/L. The independent variables are X_{tara} and shear rate (γ), corresponding to case 1 of Table 2. The error of the estimation is significantly increased when the experimental shear stress values achieve their maxima at about $X_{tara} = 0.9$. Also the error increases when γ achieves higher values. Figure 3(B) represents case 6 of Table 2. It is shown that the error is very sensitive to γ and also it is considerably higher in the neighborhood of X_{tara} 0.9. The importance of γ suggests that the estimation of the flow index (n) may be improved.

Conclusions

Experimental evidence determines that mixtures of aqueous solutions of Tara and Xanthan gum show a pseudoplastic behavior with a high synergy effect presenting a maximum viscosity value at 0.9 mass fraction of Tara gum in the concentration range from 1.0 to 4.0 g/L. The mixture synergy index ranges from 14 to 26, depending on the total concentration of the gums in solution.

This work proposes the estimation of yield stress of pure components and their mixtures by doubling the shear stress corresponding to a shear rate of 3.0 s^{-1} and subtracting the shear stress that belongs to the 9.0 s^{-1} shear rate. Results showed high correlation coefficients.

Upon testing several models, the flow curves of Tara gum and Xanthan aqueous solutions, as well as their mixtures, were well correlated by the Herschel and Bulkley model and also by the Saasen and Ytrehus modification. The consistency index and the flow index of the Herschel and Bulkley model were linearly correlated, so estimating one of them leads to define the value of the other.

For the purpose of estimating viscosity values that have not been determined experimentally, the parameters of the Herschel and Bulkley model have to be quantitatively related to composition variables of the mixtures, such as the fraction of Tara gum and the total solid concentration. Hence, to correlate the consistency index to composition, both the Auslander model and the Chebyshev polynomial yielded accurate estimations. The error of flow curves estimation for mixtures of aqueous solutions of Tara gum and Xanthan was reduced from 9.72 % to 2.59 % applying optimization routines.

The procedure outlined in this paper offers reliable results in the estimation of flow curves for mixtures that present high synergy effects. Thus, such procedure may be immediately applied in product development and process design, since defining composition variables of the mixtures allows precise estimation of viscosity.

Acknowledgment

We acknowledge Universidad Nacional de San Agustín de Arequipa, for funding the presentation of a preliminary version of this research at the CHISA congress held in Prague, 2018.

Our gratitude to Dr. Evelyn Gutierrez Ope for contributing to the experimental work.

References

1. Ahmad, K.S., Ghotbi, C., Taghikhani, V. and Jalili, A. 2013. Correlation of Viscosity of Aqueous Solutions of Alkanolamine Mixtures Based on the Eyring's Theory and Wong-Sandler Mixing Rule. *Iranian Journal of Chemistry and Chemical Engineering* 32 (2):2, 9-17.
2. Alghooneh, A., Behrouzian, F. and Razavi, S. M. A. 2019. *Hydrocolloids Interaction Elaboration Based on Rheological Properties in: Razavi, S. M. A., (Ed), First Edition. John Wiley & Sons Ltd.*
3. Allouche, M.H., Botton, V., Henry, D., Millet, S., Usha, R. and Ben Hadid, H. 2015. Experimental determination of the viscosity at very low shear rate for shear thinning fluids by electrocapillarity. *Journal of Non-Newtonian Fluid Mechanics* 215: 60-69. <http://dx.doi.org/10.1016/j.jnnfm.2014.11.003>
4. Amundarain, J. L., Castro, L. J., Rojas, M. R., Siquier, S., Ramírez, N., Müller A. J. and Sáez, A. E. 2009. Solutions of xanthan gum/guar gum mixtures: shear rheology, porous media flow, and solids transport in annular flow. *Rheologica Acta* 48: 491–498. <https://doi.org/10.1007/s00397-008-0337-5>
5. Auslander, G. 1964. Prediction of the McAllister model parameters from pure component properties for liquid binary nalkane systems, *British Chemical Engineering* 9:610–618.
6. Belda, R., Herraiz, J.V. and Diez, O. 2004. Rheological study and thermodynamic analysis of the binary system (water/ethanol): influence of concentration. *Physics and Chemistry of Liquids* 42(5):467–479.
7. Cross, M. M. 1979. Relation between viscoelasticity and shear-thinning behaviour in liquids. *Rheologica Acta* 18: 609–614.
8. Contreras-Lozano, K.P., Ciro-Velasquez, H.J. and Márquez-Cardozo, C.J. 2018. Effect of the addition of hydrocolloids and aloe vera gel (*Aloe barbadensis Miller*) on the rheological properties of a beverage of sweet corn (*Zea mays* var. saccharata). *DYNA*, 85(204), pp. 302-310. <http://dx.doi.org/10.15446/dyna.v85n204.63205>
9. Da-Lozzo, E. J., Moledo, R. C. A., Faraco, C. D., Ortolani-Machado, C. F., Bresolin, T. M. B. and MeiraSilveira, J. L. 2013 Curcumin/xanthan–galactomannan hydrogels: Rheological analysis and biocompatibility. *Carbohydrate Polymers* 93(1):279-284. <https://doi.org/10.1016/j.carbpol.2012.02.036>

10. Eberhard, U., Seybold, H. J., Floriancic, M., Bertsch, P., Jiménez-Martínez, J., Andrade, J. S. and Holzner, M. 2019. Determination of the effective viscosity of Non-newtonian Fluids Flowing Through Porous Media. *Frontiers in Physics* 7:71. <https://doi.org/10.3389/fphy.2019.00071>
11. EFSA ANS Panel (EFSA Panel on Food Additives and Nutrient Sources added to Food), Mortensen, A., Aguilar, F., Crebelli, R., Di Domenico, A., Frutos, M. J., Galtier, P., Gott, D. and Gundert-Remy, U. 2017. Scientific opinion on the re-evaluation of Tara gum (E 417) as a food additive. *EFSA Journal* 15(6):4863, 37. <https://doi.org/10.2903/j.efsa.2017.4863>
12. Falguera, V. and Ibarz, A. 2010. A New Model to Describe Flow Behavior of Concentrated Orange Juice. *Food Biophysics* 5:114–119. <https://doi.org/10.1007/s11483-010-9151-6>
13. Fitzsimons, S. M., Tobin, J. T. and Morris, E. R. 2008. Synergistic binding of konjac glucomannan to xanthan on mixing at room temperature. *Food Hydrocolloids* 22:36–46.
14. Gayathri, A., Venugopal, T. and Venkatramanan, K. 2019. Redlich-Kister coefficients on the analysis of physico-chemical characteristics of functional polymers. *Materials Today: Proceedings* 17 (4):2083-2087 ISSN 2214-7853. <https://doi.org/10.1016/j.matpr.2019.06.257>
15. Gomez- Díaz, D., Navaza, J. M. and Quintans-Riveiro, L. C. 2008. Influence of mixing and temperature on the rheological properties of carboxymethyl cellulose/j-carrageenan mixtures. *Eur Food Res Technol* 227: 1397–1402 <https://doi.org/10.1007/s00217-008-0858-2>
16. Grunberg, L. and Nissan, A. 1949. Mixture law for viscosity. *Nature* 164:799–800.
17. Gulrez, S. K. H., Al-Assaf, S., Fanga, Y., Phillips, G. O. and Gunninga, A. P. 2012. Revisiting the conformation of xanthan and the effect of industrially relevant treatments. *Carbohydrate Polymers* 90:1235–1243 <http://dx.doi.org/10.1016/j.carbpol.2012.06.055>
18. Herschel, W. H. and Bulkley, R. (1926). Measurement of consistency as applied to rubber benzene solutions. *Proceedings ASTM Part II* 26: 621–629.
19. Jo, W., Ha Bak, J. and Yoo, B. 2018. Rheological characterizations of concentrated binary gum mixtures with xanthan gum and galactomannans. *International Journal of Biological Macromolecules* 114:263-269. <https://doi.org/10.1016/j.ijbiomac.2018.03.105>
20. Kazunori, Y. 2006. A multimode viscosity model and its applicability to Non-Newtonian fluids. *Journal of Textile Engineering* 52(4):171-173.
21. Kennedy, J. R. M., Kent, K.E. and Brown, J.R. 2015. Rheology of dispersions of xanthan gum, locust bean gum and mixed biopolymer gel with silicon dioxide nanoparticles. *Materials Science and Engineering: C* 48:347-353. <https://doi.org/10.1016/j.msec.2014.12.040>
22. Knežević-Stevanović, A. B., Babić, G.M., Kijevčanin, M. L., Šerbanović, S. P. and Grozdanić D. K. 2012. Correlation of the liquid mixture viscosities. *Journal of the Serbian Chemical Society* 77(8): 1083–1089. <https://doi.org/10.2298/JSC120127038K>
23. Kim, S. H. 2014. Some properties of Chebyshev polynomials. *Journal of Inequalities and Applications* 167: 1-10.
24. Lapuerta, M., Rodríguez-Fernández, J., Fernández-Rodríguez, D. and Patiño-Camino, R. 2017. Modeling viscosity of butanol and ethanol blends with diesel and biodiesel fuels. *Fuel* 199:332–338
25. Martín-Alfonso, J. E., Cuadri, A. A., Berta, M. and Stading, M. 2018. Relation between concentration and shearextensional rheology properties of xanthan and guar gum solutions. *Carbohydrate Polymers* 181(1): 63-70. <https://doi.org/10.1016/j.carbpol.2017.10.057>
26. Moraes, I. C.F., Fasolin, L. H., Cunha, R. L., Menegalli, F.C. 2011. Dynamic and steady-shear rheological properties of Xanthan and Guar Gums dispersed in Yellow Passion fruit pulp (*Passiflora edulis f. flavicarpa*). *Brazilian Journal of Chemical Engineering* 28(3): 483 – 494.
27. Picout, D. R., Ross-Murphy, S. B. 2003. Rheology of biopolymer solutions and gels. *The Scientific World Journal* 3:105–121.
28. Ramos, F. and Hernandez, I. (2020) In: Galindo-Rosales, F. J. et al. (eds.): *Proceedings of the Iberian Meeting on Rheology (IBEREO 2019)*. Springer Nature Switzerland. 2020. https://doi.org/10.1007/978-3-030-27701-7_24
29. Rao, M. A. 2014. Rheology of fluid, semisolid, and solid foods. *Food Engineering Series*, Springer Science+Business Media New York 2014 https://doi.org/10.1007/978-1-4614-9230-6_2
30. Razavi, S. M. A., Alghooneh, A. and Behrouzian, F. 2018. Thermo-rheology and thermodynamic analysis of binary biopolymer blend: a case study on sage seed gum-xanthan gum blends. *Food Hydrocolloids* 77: 307–321. <https://doi.org/10.1016/j.foodhyd.2017.10.007>
31. Redlich, O. and Kister, A. 1948. Algebraic representation of thermodynamic properties and the classification of solutions. *Industrial and Engineering Chemistry* 40:345–348.
32. Roegiers, M. and Zhmud, B. 2011. Property blending relationships for binary mixtures of mineral oil and elektrionised vegetable oil: viscosity, solvent power, and seal compatibility index. *Lubrication Science* 23:263–278.
33. Saasen, A. and Ytrehus, J. D. 2018. Rheological Properties of Drilling Fluids: Use of dimensionless shear rates in HerschelBulkley and Power-law models. *Applied Rheology* 28 <https://doi.org/10.3933/AppIRheol-28-54515>
34. Salehi, F. and Kashaninejad, M. 2017. Effect of drying methods on textural and rheological properties of basil seed gum. *International Food Research Journal* 24(5): 2090-2096.

35. Shaari, N. A., Sulaiman, R. and Cheok, C.Y. 2017. Rheological properties of native and modified corn starches in the presence of hydrocolloids. *International Food Research Journal* 24(5): 2082-2089.
36. Scipy.org 2021. Scipy optimized least squares. Retrieved on march 09 2021 from Scipy Website: https://docs.scipy.org/doc/scipy/reference/generated/scipy.optimize.least_squares.html#scipy.optimize.least_squares
37. Secouard, S., Grisel, M. and Malhiac, C. 2007. Flavor release study as a way to explain xanthan–galactomannan interactions. *Food Hydrocolloids* 21: 1237–1244. <https://doi.org/10.1016/j.foodhyd.2006.07.011>
38. Sittikijyothin, W., Torres, D. and Goncalves, M. 2005. Modelling the rheological behaviour of galactomannan aqueous solutions. *Carbohydrate Polymers* 59:339–350
39. Souza-Mendes, P. R. and Dutra, E. S. S. 2004. Viscosity function for yield-stress liquids. *Applied Rheology* 14:296-302.
40. Soto-Caballero, M. C., Valdez-Fragoso, A., Salinas-Lopez, A. N., Welti-Chanes, J., Verardo, V. and Mujica-Paz, H. 2016. Rheological parameters of xanthan gum / pectin solutions as a function of temperature and composition. *Revista Mexicana de Ingeniería Química* 15(3):859-868
41. Tako, M. 1991. Synergistic interaction between Xanthan and Tara-Bean gum. *Carbohydrate Polymers* 16:239-252.
42. Tako, M., Teruya T., Tamaki, Y. and Ohkawa, K. 2010. Co-gelation mechanism of xanthan and galactomannan. *Colloid Polymer Science* 288:1161–1166. <https://doi.org/10.1007/s00396-010-2242-6>
43. Thompson, W. J. 1994. Chebyshev Polynomials: after the spelling the rest is easy. *Computers in physics* 8(2): 161-165.
44. Valenta, T., Lapčíková, B. and Lapčík, L. 2018. Determination of kinetic and thermodynamic parameters of food hydrocolloids/water interactions by means of thermal analysis and viscometry. *Colloids and Surfaces A: Physicochemical and Engineering Aspects* 555: 270-279. <https://doi.org/10.1016/j.colsurfa.2018.07.009>
45. Wu, Y., Li, W., Cui, W., Eskin, N. A. M. and Goff, H.D. 2012. A molecular modeling approach to understand conformation–functionality relationships of galactomannans with different mannose/galactose ratios. *Food Hydrocolloids* 26(2):359-364. <https://doi.org/10.1016/j.foodhyd.2011.02.029>
46. Wu, Y., Ding, W., Jia, L., He and Q. 2015. The rheological properties of tara gum (*caesalpinia spinosa*). *Food Chemistry* 168:366.
47. Wu, Y., Ding, W. and He, Q. 2017. Molecular characteristics of Tara galactomannans: effect of degradation with hydrogen peroxide, *International Journal of Food Properties* 20(12):3014-3022. <https://doi.org/10.1080/10942912.2016.1270300>
48. Zamora, M. and Power, D. 2002. Making a case for AADE hydraulics and the Unified Rheological Model. AADE Technology Conference “Drilling & Completion Fluids and Waste Management” AADE-02-DFWM-HO-13.
49. Zhmud, B. 2014. Viscosity blending equations. *Lube magazine* 121: 22-27.